ISBN: 978-3-95450-238-7 ISSN: 2226-0358 doi:10.18429/JACoW-ICALEPCS2023-MO3BC005

# ONLINE MODELS FOR X-RAY BEAMLINES USING SIREPO-BLUESKY

B. Nash*, D. Abell, M. Keilman, P. Moeller, I. Pogorelov, RadiaSoft LLC, Boulder, Colorado, USA
Y. Du, A. Giles, J. Lynch, T. Morris, M. Rakitin, A. Walter,
NSLS-II, Brookhaven National Lab, Upton, New York, USA
N. Goldring, State 33 Inc., Portland, Oregon, USA

*Abstract*

Synchrotron radiation beamlines transport X-rays from the electron beam source to the experimental sample. Precise alignment of the beamline optics is required to achieve adequate beam properties at the sample. This process is often done manually and can be quite time consuming. Further, we would like to know the properties at the sample in order to provide metadata for X-ray experiments. Diagnostics may provide some of this information but important properties may remain unmeasured. In order to solve both of these problems, we are developing tools to create fast online models (also known as digital twins). For this purpose, we are creating reduced models that fit into a hierarchy of X-ray models of varying degrees of complexity and runtime. These are implemented within a software framework called Sirepo-Bluesky that allows for the computation of the model from within a Bluesky session which may control a real beamline. This work is done in collaboration with NSLS-II. We present the status of the software development and beamline measurements including results from the TES beamline. Finally, we present an outlook for continuing this work and applying it to more beamlines at NSLS-II and other synchrotron facilities around the world.

## INTRODUCTION

X-rays in synchrotron light sources or XFELs are produced by an electron beam radiating during passage through a magnetic field. The electron beam is stored in a storage ring or accelerated directly from a linac. In either case, there are typically substantial diagnostics to ensure that the electron beam has adequate properties to produce the required radiation. One of the important technologies enabling this well-controlled electron beam is the use of online models in which a physics model of the beam dynamics is coupled to beam diagnostics such that the physics model is continuously updated to match the measurements. A similar technology is typically not used on the photon beam. With increased X-ray brightness and coherence in both synchrotron light sources and XFELs, we propose to develop the tools to enable this technology.

There are several pieces required to implement an online model. One needs the reduced models to describe the beam propagation and one needs a software framework to integrate this into the beamline control system. Here we present further progress in the development of reduced models for use during real-time operation of X-ray beamlines. We also describe how these models have been integrated into the Sirepo framework that includes interfaces to the full X-Ray beamline simulation codes such Shadow [1] and SRW [2, 3].

A related technology for beamline control that we are developing is that of Bayesian Optimization. Here, the measured beam is directly related to beamline control parameters such as mirror positions or slit settings. A probabilistic model based on Gaussian processes is then used to directly optimize the measured beam distribution. This is a very effective approach to automate beamline alignment and reconfiguration, even if the resulting model is less interpretable. We describe substantial progress in this approach, as it fits into the same software ecosystem including Sirepo-Bluesky.

In [4], we introduced the concept of a matrix-aperture beamline composed of linear transport sections and physical apertures as shown in Fig. 1. This approach is an approximation with the hope of capturing important transport properties in a computationally efficient manner. Within this approach, there exists a hierarchy of methods [1] as shown in Fig. 2. The first row of the table involves second-moment propagation representing Gaussian Wigner functions [6]. The second row of the table involves propagating coherent electric fields via linear canonical transform (LCT). Progress in the creation of an LCT transport library is reported in [7]. The final row of the table represents generic partially coherent X-ray propagation via Wigner function passing through the matrix-aperture beamline. Some work towards developing this method was presented in [8]. The focus of this paper will be the top-level method of sigma matrix transport through the matrix-aperture beamline. We refer to this reduced model as the Gaussian Wigner function moment (GWFM) model. This model provides a computationally efficient calculation of the linear optics through the beamline, while also including effects of partial coherence. We apply the sigma matrix transport method to a KB mirror beamline with two apertures and compare results with SRW and Shadow. Finally, the realistic case of an NSLS-II beamline is treated with this method, and preliminary results are presented.

We remind the reader that the goal of such fast reduced models is to enable the creation of online models incorporating up-to-the-moment diagnostics data such that the model accurately reflects the true state of the beamline settings and X-ray transport from source to sample. Such an online model

* bnash@radiasoft.net

[1] We do not intend to be comprehensive in our scope of all work pertaining to reduced models here. The hybrid method [5] may fit closely within our schema as an alternative to the LCT method, combining wavefront propagation with ray tracing.

ISBN: 978-3-95450-238-7 ISSN: 2226-0358 doi:10.18429/JACoW-ICALEPCS2023-MO3BC005

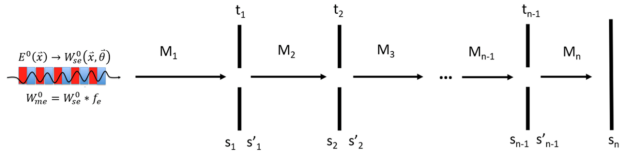


Figure 1: Matrix-aperture beamline schematic with $n$ linear transport sections and $n-1$ apertures. $M_j$ represents the transport matrix across the $j^{\text{th}}$ section of the beamline (from position $s_{j-1}$ to $s_j$), and $t_j$ represents the transfer function of the $j^{\text{th}}$ aperture. An undulator source is depicted in this figure creating partially coherent synchrotron radiation.

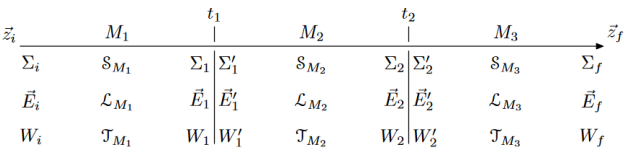


Figure 2: Hierarchy of reduced models for radiation transport through a matrix-aperture beamline.

may be used to automate precise tuning and alignment of the beamline. In addition to physics-based models, we are also developing machine learning-based models for the same purpose. See [9] for further information on the progress of this effort.

## ONLINE AND REDUCED MODELS

An online model is a model that runs in real time, in parallel with operations, that is updated based on diagnostics measurements. In order for such a model to be updated within reasonable synchrony with the actual changing state of the physical system, one typically requires a *reduced model*. This is a limited fidelity model with adequately fast computation speed.

Online models using models of reduced computational complexity are commonly used in particle accelerators. For a linac or a storage ring, typically one tracks the beam centroid and the beam envelope. Various formulations of the beam envelope exist, most commonly in terms of Twiss parameters and emittances.

Such a formulation has not commonly been used for the X-rays created by the electrons in synchrotron light sources and X-ray free electron lasers (XFELs). We have developed such a reduced model for partially coherent radiation, in terms of a Gaussian Wigner function with a varying centroid similar to the orbit of a particle beam. This has been integrated into the Sirepo interface to the SHADOW code and is available as the "beam statistics report". We have also developed a library for the Linear Canonical Transform reduced model that we describe here. This has not yet been integrated with Sirepo and SHADOW.

## SIREPO-BLUESKY

The Sirepo-Bluesky library provides an interface between the Bluesky experimental orchestration library and the simulation tools available within Sirepo. A diagram showing the relationship between Sirepo with its simulation tools, Bluesky with its ability to orchestrate X-ray experiments and the EPICS control software is presented in Fig. 3.

A recent proceedings paper [10] on the Sirepo-Bluesky library can be read for further details.

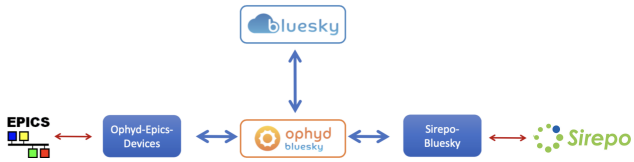


Figure 3: Diagram showing the relationship between software components within an online model for an X-ray beamline.

## GAUSSIAN WIGNER FUNCTION REDUCED MODEL

The Gaussian Wigner function approach is more fully outlined elsewhere [11]. Here we give a brief overview and demonstrate its use on a Kirkpatrick-Baez mirror beamline with an aperture.

Radiation for synchrotron light sources is partially coherent, resulting from the different electrons with a random longitudinal distribution emitting independently. In XFELs, the electron beam becomes micro-bunched and the radiation is closer to fully coherent. The radiation can be described with statistical optics and in many cases a good appriximation is given by the Gauss-Schell model. Equivalent to the Gauss-Schell model is a Gaussian Wigner function.

We consider the case of a KB mirror beamline with successive horizontally and vertically focusing mirrors as shown in Fig. 4. We have setup this beamline within the Shadow code to illustrate the method of moment propagation through a matrix-aperture beamline. The transfer matrices along the beamline are computed as described in [4]. In addition, we introduce a rectangular aperture 14 meters from the source. The horizontal and vertical sizes of an aperture in Shadow are represented by the variables `RX_SLIT` and `RY_SLIT` respectively and correspond to $2a_h$ within our analysis [6]. As discussed therein, the Gaussian aperture size, $a_g$, is proportional to the hard-edge aperture size, $a_h$, with the proportionality factor weakly dependent on beam parameters (details are currently under study). For this work, we assumed $a_g = a_h$.

For this study, we define an initial beam size of 45 µm in the horizontal and 25 µm in the vertical and consider a wavelength, $\lambda$, of 1.24 nm corresponding to an energy of 1 keV. We define the divergences according to the following equation:

$$\sigma_{x,y}\sigma_{\theta_{x,y}} = m^2_{x,y}\frac{\lambda}{4\pi} \tag{1}$$

where $m^2_{x,y}$ is known as the beam quality factor in the optics literature. $m_{x,y} = 1$ represents the coherent case and $m_{x,y} >$

ISBN: 978-3-95450-238-7 ISSN: 2226-0358 doi:10.18429/JACoW-ICALEPCS2023-M03BC005

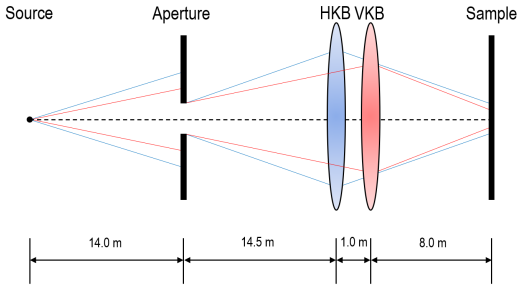


Figure 4: Diagram of KB-mirror beamline with beam defining aperture. Blue and red lines represent horizontal and vertical beam projection respectively. HKB and VKB are horizontally and vertically focusing elliptical mirrors represented by lenses in the diagram.

1 represents the partially coherent case. For the coherent case, the divergences are $\sigma_{\theta_x} = 2.2$ µrad and $\sigma_{\theta_y} = 3.9$ µrad. In the partially coherent case, the divergences will be larger.

We propagate this beam in the highly but not fully coherent case of $m_x^2 = m_y^2 = 1.1$. The beam size evolution with rectangular hard-edge aperture of size $a_{h_x} = 50$ µm and $a_{h_y} = 45$ µm is shown in Fig. 5.

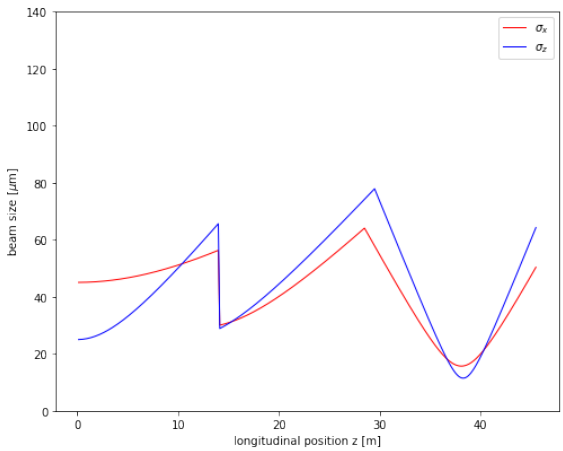


Figure 5: Horizontal ($\sigma_x$) and vertical ($\sigma_z$) X-ray beam size evolution through KB beamline with Gaussian aperture.

Next we consider the evolution of the photon beam emittance which is defined analogously to the quantity in beam dynamics as

$$\epsilon = \sqrt{\sigma_{xx}\sigma_{\theta_x\theta_x} - \sigma_{x\theta_x}^2}\,. \tag{2}$$

The evolution of the emittance down the KB aperture beamline is shown in Fig. 6 for increasing value of beam quality factor. We first note that linear sections preserve the emittance. In the coherent case, the emittance is also conserved across the aperture. However, as the coherence decreases, one finds that the emittance decreases more and more across the aperture.

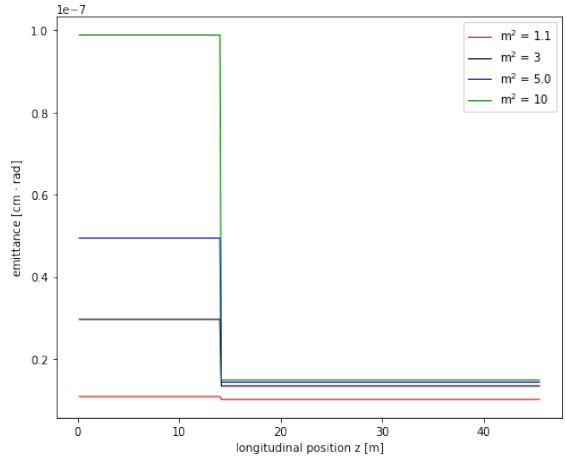


Figure 6: Evolution of horizontal X-ray beam emittance through KB-mirror aperture beamline with varying values of beam quality factor.

## LINEAR CANONICAL TRANSFORM

The *Linear Canonical Transform*, or LCT, encompasses a wide range of integral transforms used in mathematical physics, including Fresnel and Fourier transforms. Here, we describe the LCT of functions in one and two degrees of freedom. And we describe and test algorithms for the fast numerical computation of LCTs. The LCT arose independently in the contexts of optics [12] and quantum mechanics [13, 14]. See also Wolf's historical remarks in [15, Ch. 1]. For the optical context of immediate interest to us, the LCT relates the electric field at the image plane, $E(x)$, to that at the object plane, $E_0(x)$. In one degree of freedom, with the linear optics described by the *symplectic* ray optical matrix $M = \left(\begin{smallmatrix} a & b \\ c & d \end{smallmatrix}\right)$, Collins proves [12] that

$$E(x) = \sqrt{\frac{k}{\mathrm{i}2\pi b}}\, \mathrm{e}^{\mathrm{i}kL_o} \int_{-\infty}^{\infty} \exp\Big[\frac{\mathrm{i}k}{2b}(dx^2 - 2xx_0 + ax_0^2)\Big] \times E_0(x_0)\,\mathrm{d}x_0. \tag{3}$$

Here $k = 2\pi/\lambda$ denotes the wave number of the propagating electric field, and $L_o$ the optical path length along the axis. To simplify and improve numerical aspects of the computation, we set a to-be-determined *scale length* $l$, write $x = lu$, $x_0 = lv$, and factor out the rapid $\mathrm{e}^{\mathrm{i}kz}$ phase evolution. Then the integral transform $E_0 \to E$ becomes the LCT $f_0 \to f = \mathcal{L}_{\bar{M}}[f_0]$, defined by the dimensionless—but still symplectic—matrix

$$\bar{M} = \begin{pmatrix} A & B \\ C & D \end{pmatrix} = \begin{pmatrix} a & \lambda b/l^2 \\ l^2 c/\lambda & d \end{pmatrix}, \tag{4}$$

together with the rule

$$f(u) = \mathcal{L}_{\bar{M}}[f_0](u) = \frac{1}{\sqrt{\mathrm{i}B}} \int_{-\infty}^{\infty} \exp\Big[\frac{\mathrm{i}\pi}{B}(Du^2 - 2uv + Av^2)\Big] f_0(v)\,\mathrm{d}v. \tag{5}$$

Wolf states [15] that the leading factor of $1/\sqrt{\mathrm{i}}$ "requires some care" to ensure the correct phase. In the case $B = 0$,

ISBN: 978-3-95450-238-7 ISSN: 2226-0358 doi:10.18429/JACoW-ICALEPCS2023-MO3BC005



taking the limit $B \to 0$, and making use of the fact that $\det \bar{M} = 1$, yields the result

$$f(u) = \mathcal{L}_{\bar{M}(B=0)}[f_0](u) = \mathrm{e}^{\mathrm{i}\pi(C/A)u^2} \frac{1}{\sqrt{A}} f_0\left(\frac{u}{A}\right). \quad (6)$$

In two degrees of freedom, the ray optical matrix becomes $4 \times 4$—now with $2 \times 2$ blocks labeled $A$, $B$, $C$, $D$:

$$M = \begin{pmatrix} A & B \\ C & D \end{pmatrix}. \quad (7)$$

In this context, the symplecticity of $M$ means that the $2 \times 2$ submatrices $A$, $B$, $C$, and $D$ must obey the relations [16]

$$A^{\mathrm{tr}}C = C^{\mathrm{tr}}A, \quad B^{\mathrm{tr}}D = D^{\mathrm{tr}}B, \quad A^{\mathrm{tr}}D - C^{\mathrm{tr}}B = I, \quad (8a)$$

$$AB^{\mathrm{tr}} = BA^{\mathrm{tr}}, \quad CD^{\mathrm{tr}} = DC^{\mathrm{tr}}, \quad AD^{\mathrm{tr}} - BC^{\mathrm{tr}} = I, \quad (8b)$$

where the tilde ($\square^{\mathrm{tr}}$) denotes matrix transposition, and $I$ denotes the $2\times2$ identity matrix. Then the 2D LCT is defined by the rule (see, for example, [16] or [15])

$$\begin{aligned} f(\vec{u}) &= \mathcal{L}_{\bar{M}}[f_0](\vec{u}) \\ &= \frac{1}{\sqrt{\det \mathrm{i}B}} \int_{-\infty}^{\infty} \int_{-\infty}^{\infty} \exp[\mathrm{i}\pi p(\vec{u},\vec{v})] f_0(\vec{v})\, \mathrm{d}^2\vec{v}, \end{aligned} \quad (9)$$

with $p$ the quadratic form

$$p(\vec{u},\vec{v}) = \vec{u}^{\mathrm{tr}} D B^{-1} \vec{u} - 2\vec{v}^{\mathrm{tr}} B^{-1} \vec{u} + \vec{v}^{\mathrm{tr}} B^{-1} A \vec{v}. \quad (10)$$

(As in the 1D case, the phase of that leading factor "requires some care".) *N.B:* The fact that the submatrices $A$, $B$, $C$, $D$ obey the particular relations given above tells us that the matrix $M$ acts on phase-space variables given in the order $(q_1, q_2, p_1, p_2)$ (see, for example, [17, §3.3]). This means that if one extracts the ray optical matrix $M$ with the phase-space variables given in some other order, *e.g.* $(q_1, p_1, q_2, p_2)$, then one must—for the purposes of the computation described here—make sure to permute appropriately the matrix entries of $M$ before assigning the $2 \times 2$ entries $A$, $B$, $C$, and $D$. In both one and two degrees of freedom, the LCT obeys the very important *group property* [18]

$$\mathcal{L}_{M_2 \cdot M_1} = \mathcal{L}_{M_2} \circ \mathcal{L}_{M_1}. \quad (11)$$

As a consequence, one may compute a given LCT as a composition of simpler LCTs. And this is the mechanism behind the construction of fast algorithms for LCTs. The algorithms given by [16], and by [19], first decompose the symplectic matrix defining a given LCT into a product of simpler symplectic matrices. In one degree of freedom, those simpler matrices define specific special cases of the LCT: scaling, chirp multiplication, and Fourier transform. The above group property allows one to write any LCT as a corresponding composition of those simpler transforms. Because chirp multiplication enlarges the *effective* time-bandwidth product, we must also, at some points in the computation, resample the signal.

- The operation of *scaling* corresponds to an LCT with matrix

$$M_m = \begin{pmatrix} m & 0 \\ 0 & 1/m \end{pmatrix}. \quad (12)$$

Its acts on a function $f(u)$ according to the rule

$$[\mathcal{M}_m f](u) = \frac{1}{\sqrt{m}} f\left(\frac{u}{m}\right), \quad (13)$$

or, equivalently,

$$[\mathcal{M}_m f](m \cdot u) = \frac{1}{\sqrt{m}} f(u). \quad (14)$$

*NB:* If $m < 0$, then we must introduce a factor of $\pm\mathrm{i}$, with present evidence suggesting use of the positive root.

- Aside from an overall phase factor, the *Fourier transform* operation corresponds to the LCT with matrix

$$F_{\mathrm{LC}} = \begin{pmatrix} 0 & 1 \\ -1 & 0 \end{pmatrix}. \quad (15)$$

More specifically, the LC Fourier transform acts on a function $f(u)$ according to the rule

$$[\mathcal{F}_{\mathrm{LC}} f](v) = \mathrm{e}^{-\mathrm{i}\pi/4} \int_{-\infty}^{\infty} \mathrm{e}^{-\mathrm{i}2\pi uv} f(u)\, \mathrm{d}u. \quad (16)$$

In numerical work, we approximate that integral as

$$\begin{aligned} \int_{-\infty}^{\infty} \mathrm{e}^{-\mathrm{i}2\pi uv} f(u)\, \mathrm{d}u &\approx \int_{-P/2}^{P/2} \mathrm{e}^{-\mathrm{i}2\pi uv} f(u)\, \mathrm{d}u \\ &\approx \frac{P}{N} \sum_j^N \mathrm{e}^{-\mathrm{i}2\pi jk/N} f\left(j\frac{P}{N}\right). \end{aligned} \quad (17)$$

- The operation of *chirp multiplication* corresponds to an LCT with matrix

$$Q_q = \begin{pmatrix} 1 & 0 \\ -q & 1 \end{pmatrix}. \quad (18)$$

Its acts on a function $f(u)$ according to the rule

$$[\mathcal{Q}_q f](u) = \mathrm{e}^{-\mathrm{i}\pi q u^2} f(u). \quad (19)$$

The relation between the symplectic $2 \times 2$ matrix $M$ and the parameters $(\alpha, \beta, \gamma)$ (used by [16] and others) is given by the relation

$$\begin{pmatrix} A & B \\ C & D \end{pmatrix} = \begin{pmatrix} \gamma/\beta & 1/\beta \\ \alpha\gamma/\beta - \beta & \alpha/\beta \end{pmatrix}, \quad (20)$$

or the inverse relations

$$\alpha = D/B, \quad \beta = 1/B, \quad \gamma = A/B. \quad (21)$$

Because this representation does not handle gracefully the case $B = 0$, we point out that

$$\bar{M} = \begin{pmatrix} A & 0 \\ C & D \end{pmatrix} = \begin{pmatrix} A & 0 \\ C & 1/A \end{pmatrix} = \begin{pmatrix} 1 & 0 \\ C/A & 1 \end{pmatrix} \begin{pmatrix} A & 0 \\ 0 & 1/A \end{pmatrix}. \quad (22)$$

ISBN: 978-3-95450-238-7 ISSN: 2226-0358 doi:10.18429/JACoW-ICALEPCS2023-M03BC005

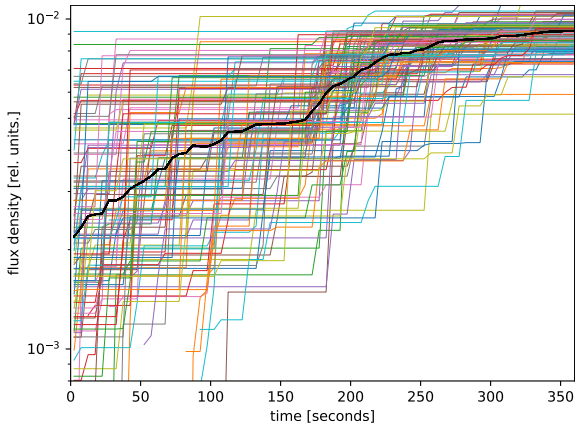


Figure 7: Convergence plot of six-dimensional optimization for the NSLS-II TES beamline.

In words, this result says that for the case $B = 0$ one applies a scaling by factor $A$ followed by a chirp multiplication by factor $-C/A$.

The above work—still under development—is now incorporated into the publicly available GitHub repository rsmath.[2]

## BAYESIAN OPTIMIZATION

The reduced physics models we have described including the Gaussian Wigner function and the Linear Canonical Transform may be used in online models for X-ray beamlines by matching their parameters to observations at beam diagnostics. In addition to being able to use these models for beamline optimization, as shown in Fig. 7, they also provide the operator important understanding of the state of the beamline, allowing human-in-the-loop optimization.

A more direct approach to beamline optimization using diagnostics forgoes the use of physics models and instead uses a probabilistic approach where inputs and outputs are directly modeled via a Gaussian process, and decisions for beamline measurements are made based on a corresponding Bayesian framework.

We have developed a Bayesian optimization toolbox for beamline alignment called bloptools[3] that establishes an interface between Bluesky and the BoTorch/GPyTorch libraries. Further information about this package and results for optimizing KB mirrors on the TES beamline at NSLS-II can be found in a recent proceedings paper [20].

## CONCLUSION AND OUTLOOK

We have given an update in progress towards the technical pieces required for online models of X-ray beamlines. The reduced models are needed for fast computation of the x-ray properties in conjunction with diagnostic measurements. The models are being integrated into Sirepo along with the x-ray optics codes SHADOW and SRW. A screenshot of this integration is shown in Fig. 8 where the NSLS-II TES beamline has been modeled both with Sirepo-Shadow and the Gaussian Wigner function model (beam statistics report). The Sirepo-Bluesky library then provides the link between Bluesky for operating experiments and aligning a beamline and the reduced x-ray models.

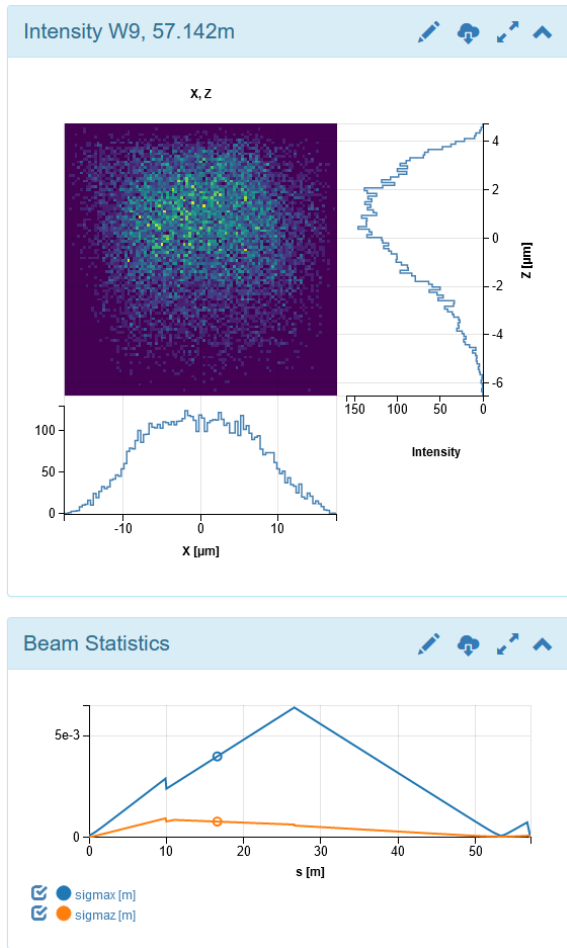


Figure 8: Final intensity plot and beam statistics report in Sirepo-Shadow interface for the NSLS-II TES beamline.

We are also developing the method of Bayesian Optimization of beamlines that uses a statistical model rather than a physics based model. The toolkit we have developed works within the framework of Sirepo-Bluesky and can thus take advantage of the virtual beamlines available in Sirepo.

We summarize some reduced models for X-ray beamlines focusing on our recent results for a Gaussian Wigner function model and demonstrating it's use for a KB beamline with aperture. These formulae have been integrated into the Shadow ray tracing code allowing for propagation of moments through realistic beamlines including focusing elements and physical apertures. For a simple KB aperture beamline, we demonstrated this method showing how beam size, emittance, and coherence length evolve down the beamline. We are in the process of integrating the GWFM model into the Sirepo-Shadow interface.

We have described how these reduced models and full

[2] https://github.com/radiasoft/rsmath
[3] https://github.com/NSLS-II/bloptools

ISBN: 978-3-95450-238-7 ISSN: 2226-0358 doi:10.18429/JACoW-ICALEPCS2023-MO3BC005



X-ray optics beamline simulation codes may be integrated within a beamline control system using the Sirepo-Bluesky software package [10, 21, 22].

The missing piece for creating online models of x-ray beamlines is benchmarking simulations from the reduced models to the measured beam properties. Just as beam position monitors (BPMs) for electron beams are used to measure the Twiss functions down a linac or in a storage ring, x-ray BPMs may do the same for the x-ray beam orbit and sizes. We hope that the theoretical and software tools we present here provide a substantial step towards the reality of online models for the many x-ray beamlines throughout the world.

## ACKNOWLEDGMENTS

The work was supported in part by the DOE SBIR project (Award No. DE-SC00020593) titled "X-ray Beamline Control with an Online Model for Automated Tuning and Reconfiguration'' and in part by BNL's LDRD-22-031 project titled "Simulation-aided Instrument Optimization using Artificial Intelligence and Machine Learning Methods''. Further support for the development of the Linear Canonical Transform library came from the DOE SBIR project (Award No. DE-SC0020931) "Integrated Multiphysics Design of High-power Short-pulse Lasers". Finally, This research used resources of the TES beamline of the National Synchrotron Light Source II, a U.S. Department of Energy (DOE) Office of Science User Facility operated for the DOE Office of Science by Brookhaven National Laboratory under Contract No. DE-SC0012704.

## REFERENCES

[1] M. Sanchez del Rio, N. Canestrari, F. Jiang, and F. Cerrina, "*Shadow3*: A new version of the synchrotron x-ray optics modelling package", *J. Synchrotron Radiat.*, vol. 18, no. 5, pp. 708–716, 2011. doi:10.1107/S0909049511026306

[2] O. Chubar and P. Elleaume, "Accurate and efficient computation of synchrontron radiation in the near field region", in *Proceedings EPAC'98*, 1998, pp. 1177–1179.

[3] O. Chubar *et al.*, "Physical optics computer code optimized for synchrotron radiation", in *Proc. SPIE*, vol. 4769, 2002, pp. 145–151.

[4] B. Nash, N. Goldring, J. Edelen, C. Federer, P. Moeller, and S. Webb, "Reduced model representation of x-ray transport suitable for beamline control", in *Adv. Comput. Methods X-Ray Opt. V*, International Society for Optics and Photonics, vol. 11493, 2020, pp. 53–61. doi:10.1117/12.2568187

[5] X. Shi, R. Reininger, M. S. Del Rio, and L. Assoufid, "A hybrid method for X-ray optics simulation: combining geometric ray-tracing and wavefront propagation", *J. Synchrotron Radiat.*, vol. 21, no. Pt, p. 4, 2014. doi:10.1107/S160057751400650X

[6] B. Nash, D. T. Abell, N. B. Goldring, P. Moeller, and I. V. Pogorelov, "Propagation of Gaussian Wigner Function Through a Matrix-Aperture Beamline", in *Proc. IPAC'22*, Bangkok, Thailand, 2022, pp. 2755–2758. doi:10.18429/JACoW-IPAC2022-THPOPT067

[7] B. Nash, D. T. Abell, N. B. Goldring, P. Moeller, and I. V. Pogorelov, "Linear Canonical Transform Library for Fast Coherent X-Ray Wavefront Propagation", in *Proc. IPAC'22*, Bangkok, Thailand, 2022, pp. 2759–2762. doi:10.18429/JACoW-IPAC2022-THPOPT068

[8] B. Nash, N. Goldring, J. Edelen, S. Webb, and R. Celestre, "Propagation of partially coherent radiation using Wigner functions", *Phys. Rev. Accel. Beams*, vol. 24, no. 1, p. 010 702, 2021. doi:10.1103/PhysRevAccelBeams.24.010702

[9] T. Morris *et al.*, "On-the-fly optimization of synchrotron beamlines using machine learning", in *Opt. Syst. Alignment Toler. Verif. XIV*, 2022.

[10] M. Rakitin *et al.*, "Recent updates of the Sirepo-Bluesky library for virtual beamline representation", in *Proc. Adv. Comput. Methods X-Ray Opt. VI*, vol. 12697, 2023, pp. 103–113. doi:10.1117/12.2678030

[11] I. V. Pogorelov, B. Nash, D. T. Abell, and P. Moeller, "Propagation of a Gaussian Wigner Function Through a Matrix-Aperture Beamline", *arXiv*, 2023. doi:10.48550/arXiv.2309.11008

[12] S. A. Collins, "Lens-system diffraction integral written in terms of matrix optics", *J. Opt. Soc. Amer.*, vol. 60, no. 9, pp. 1168–1177, 1970. doi:10.1364/JOSA.60.001168

[13] M. Moshinsky and C. Quesne, "Linear canonical transformations and their unitary representations", *J. Math. Phys.*, vol. 12, no. 8, pp. 1772–1780, 1971. doi:10.1063/1.1665805

[14] C. Quesne and M. Moshinsky, "Canonical transformations and matrix elements", *J. Math. Phys.*, vol. 12, no. 8, pp. 1780–1783, 1971. doi:10.1063/1.1665806

[15] J. J. Healy, M. A. Kutay, H. M. Ozaktas, and J. T. Sheridan, Eds., *Linear Canonical Transforms: Theory and Applications*. Springer, 2016, vol. 198.

[16] A. Koç, "Fast algorithms for digital computationof linear canonical transforms", PhD dissertation, Stanford University, 2011.

[17] Lie Methods for Nonlinear Dynamics with Applications to Accelerator Physics, http://www.physics.umd.edu/dsat/

[18] K. B. Wolf, *Integral Transforms in Science and Engineering*. Plenum Press, 1979, vol. 11. https://www.fis.unam.mx/~bwolf/integral.html

[19] A. Koç, H. M. Ozaktas, C. Candan, and M. A. Kutay, "Digital computation of linear canonical transforms", *IEEE Trans. Signal Process.*, vol. 56, no. 6, pp. 2383–2394, 2008. doi:10.1109/TSP.2007.912890

[20] T. W. Morris *et al.*, "Latent Bayesian optimization for the autonomous alignment of synchrotron beamlines", in *Proc. Adv. Comput. Methods X-Ray Opt. VI*, vol. 12697, 2023, pp. 89–96. doi:10.1117/12.2677895

[21] sirepo-bluesky, https://github.com/NSLS-II/sirepo-bluesky

[22] M. S. Rakitin *et al.*, "Introduction of the Sirepo-Bluesky interface and its application to the optimization problems", in *Proc. Adv. Comput. Methods X-Ray Opt. V*, vol. 11493, 2020, pp. 209–226. doi:10.1117/12.2569000